Spectral Domain Spline Graph Filter Bank

Amir Miraki, Hamid Saeedi-Sourck, Nicola Marchetti, and Arman Farhang, *Member, IEEE*

***Abstract*—In this letter, we present a structure for two-channel spline graph filter bank with spectral sampling (SGFBSS) on arbitrary undirected graphs. Our proposed structure has many desirable properties; namely, perfect reconstruction, critical sampling in spectral domain, flexibility in the choice of shape and cut-off frequency of the filters, and low complexity implementation of the synthesis section, thanks to our closed-form derivation of the synthesis filter and its sparse structure. These properties play a pivotal role in multi-scale transforms of graph signals. Additionally, this framework can use both normalized and non-normalized Laplacian of any undirected graph. We evaluate the performance of our proposed SGFBSS structure in nonlinear approximation and denoising applications through simulations. We also compare our method with the existing graph filter bank structures and show its superior performance.**

***Index Terms*—Graph signal processing, spectral sampling, spline graph filter bank.**

I. Introduction

GRAPH signal processing (GSP) extends classical signal processing to enable analysis of irregularly structured data on the vertices of an underlying graph, [1], [2]. In recent years, GSP has been utilized in a plethora of real-life applications such as data processing in social, transport, economic, biological and sensor networks [2]. The high dimensional nature of data in these networks necessitates multirate signal analysis by construction of filter banks on graphs for different purposes such as denoising, compression, and data classification, [3].

Graph filter banks (GFB) were first proposed for special types of graphs, namely, tree, Ω-structure, circulant, and bipartite graphs [4]–[7]. The authors in [7] proposed a two-channel critically-sampled GFB structure with quadrature mirror filters (GraphQMF) satisfying the perfect reconstruction (PR) property for signals on bipartite graphs. This method is applicable to any arbitrary graph through a bipartite subgraph decomposition leading to a high computational complexity. Alternative filter design methods for the GFB structure in [7] with biorthogonal and frequency conversion based filters were proposed in [8] and [9], known as GraphBior and GraphFC, respectively. An M-channel oversampled extension of [7] was presented in [10]. In a more recent work, [11], the results of [7] are extended to arbitrary graphs, without the need for bipartite subgraph decomposition, using a different definition of the graph Fourier transform (GFT). The authors in [12] decomposed an arbitrary graph into several subgraphs. They applied a local GFT to each subgraph and obtained a GFB with PR property (SubGFB). An M-channel critically sampled GFB (CSFB) on arbitrary graphs was introduced in [13], where the synthesis filters in each subband were replaced with interpolation operators. Authors in [14] proposed a critical sampling method for two-channel filter bank on an arbitrary graph where the PR condition was only satisfied for bipartite graphs. Another GFB for arbitrary graphs is the spline graph filter bank (SGFB) [15]. The key difference between SGFB and other GFB structures is in the substitution of synthesis filters with an inverse filter, which simplifies the GFB design, see Fig. 1.

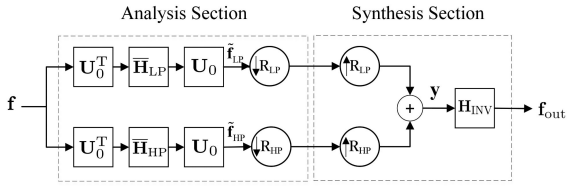

Fig. 1. Two-channel SGFB with vertex sampling [15].

Unlike classical filter banks, a down/upsampled signal in GFB has a considerably different spectrum from that of the original signal, except for bipartite graphs [16], [17]. This is a big challenge for multiscale analysis and processing on arbitrary graphs. To deal with this challenge, different approaches have emerged, [18]–[21]. The authors in [18] and [19] proposed a GFB structure without down/upsampling that leads to a large computational load. In contrast, the authors in [20] and [21], take a more interesting approach and perform down/upsampling operations in the spectral domain. This idea led to a critically-sampled GFB structure with spectral sampling (GraphSS) that is applicable to arbitrary graphs while satisfying the PR condition. The concept of spectral sampling, its superior performance to vertex domain methods, [16], and the results of [20] and [21] are among the main motivations for extending SGFB, [15], from vertex domain to spectral domain in this letter. In [15], the designed analysis filters do not have desirable passband/stopband characteristics. Hence, a filter design method, known as modified SGFB (MSGFB), was proposed in [22]. However, SGFB has a number of limitations; namely, change in the spectral shape of the signal due to vertex domain down/upsampling for arbitrary graphs, deteriorated performance compared to spectral sampling-based GFBs, and a high computational load due to the dense matrix inversion and multiplication operations at the synthesis section. Thus, the main goal of this letter is to address all these limitations.

Our main contributions in this letter are the following; (i) We propose a structure for two-channel SGFB with spectral sampling (SGFBSS) on arbitrary undirected graphs, see Fig. 2. (ii) We derive the PR conditions for this structure and show that

Manuscript received November 23, 2020; revised January 31, 2021; accepted February 6, 2021. Date of publication February 12, 2021; date of current version March 10, 2021. The associate editor coordinating the review of this manuscript and approving it for publication was Prof. Mylene Q. Farias *(Corresponding author: Hamid Saeedi-Sourck.)*

Amir Miraki and Hamid Saeedi-Sourck are with the Department of Electrical Engineering, Yazd University, Yazd 89158-18411, Iran (e-mail: amir.miraki@stu.yazd.ac.ir; saeedi@yazd.ac.ir).

Nicola Marchetti is with the Trinity College Dublin, Dublin Dublin 2, Ireland (e-mail: nicola.marchetti@tcd.ie).

Arman Farhang is with the Maynooth University, Maynooth W23 F2H6, Ireland (e-mail: arman.farhang@mu.ie).

Digital Object Identifier 10.1109/LSP.2021.3059203

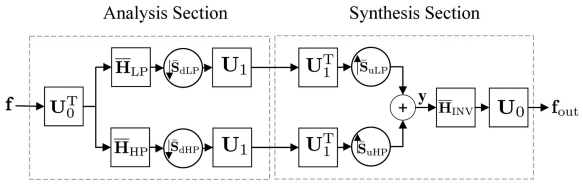

Fig. 2. Proposed two-channel SGFB with spectral sampling.

they are satisfied for arbitrary graphs without the need for any subgraph partitioning or decomposition. (iii) We derive a closed-form expression for the inverse filter at the synthesis side that is sparse and hence it leads to a low complexity implementation. Our proposed SGFBSS structure has the following desirable advantages. It can use both normalized and non-normalized graph Laplacian. Since down/upsampling operations are performed in the spectral domain, they preserve the spectral shape of the signal. Based on the derived PR conditions, we present the filter design methodology and show that our proposal provides a large amount of flexibility in the choice of filter parameters, e.g., their shape and cut-off frequency. Our numerical results demonstrate the effectiveness of the proposed SGFBSS structure for applications such as nonlinear approximation and denoising on arbitrary undirected graphs. We compare our method with the existing GFB structures in the literature and show its superior performance.

Notations and preliminaries: Boldface uppercase, boldface lowercase and normal letters represent matrices, vectors and scalar quantities, respectively. The superscript $(\cdot)^{\mathrm{T}}$ denotes the transpose operation. A graph $\mathcal{G} = (\mathcal{V}, \mathcal{E})$ is defined with a set of nodes $\mathcal{V}$, a set of edges $\mathcal{E}$ and an adjacency matrix $\mathbf{A}$ that describes the graph connectivity. $\mathbf{D}$ is the diagonal degree matrix whose diagonal elements are defined as the sum of the elements on the respective row of $\mathbf{A}$. In this letter, we consider undirected graphs without self-loops, i.e., the elements on the main diagonal of $\mathbf{A}$ are all zero. The graph Laplacian matrix is defined as $\mathbf{L} \equiv \mathbf{D} - \mathbf{A}$. Normalized adjacency and Laplacian matrices are defined as $\boldsymbol{\mathcal{A}} \equiv \mathbf{D}^{-1/2}\mathbf{A}\mathbf{D}^{-1/2}$ and $\boldsymbol{\mathcal{L}} \equiv \mathbf{D}^{-1/2}\mathbf{L}\mathbf{D}^{-1/2} = \mathbf{I}_N - \boldsymbol{\mathcal{A}}$, respectively, where $\mathbf{I}_N$ is the $N \times N$ identity matrix. For connected graphs, $\boldsymbol{\mathcal{L}}$ is a real-valued symmetric matrix. Thus, using eigenvalue decomposition, it can be written as $\boldsymbol{\mathcal{L}} = \mathbf{U}\boldsymbol{\Lambda}\mathbf{U}^{\mathrm{T}}$, where $\boldsymbol{\Lambda} = \mathrm{diag}([\lambda_0, \ldots, \lambda_{N-1}]^{\mathrm{T}})$ is the diagonal eigenvalue matrix with the diagonal elements $0 = \lambda_0 < \lambda_1 \leq \cdots \leq \lambda_{N-1} \leq 2$, $\mathbf{U} = [\mathbf{u}_0, \ldots, \mathbf{u}_{N-1}]$ is a unitary matrix that contains the orthonormal eigenvectors $\mathbf{u}_n$ on its columns and $\mathbf{U}\mathbf{U}^{\mathrm{T}} = \mathbf{I}_N$. Considering the signal $\mathbf{f} = [f(0), \ldots, f(N-1)]^{\mathrm{T}}$ where the sample $f(n)$ appears on the nth node of the graph, GFT of this signal is defined as $\bar{\mathbf{f}} \triangleq \mathbf{U}^{\mathrm{T}}\mathbf{f}$. Equivalently, inverse GFT of $\bar{\mathbf{f}}$ can be obtained as $\mathbf{f} = \mathbf{U}\bar{\mathbf{f}}$. Finally, the filtered signal is expressed as $\tilde{\mathbf{f}} = \mathbf{H}\mathbf{f}$, where $\mathbf{H} = \mathbf{U}\,\overline{\mathbf{H}}\mathbf{U}^{\mathrm{T}}$ and the filter kernel $\overline{\mathbf{H}}$ is a diagonal matrix with the elements $\bar{H}(n)$ on its main diagonal, i.e., $\overline{\mathbf{H}} = \mathrm{diag}([\bar{H}(0), \ldots, \bar{H}(N-1)]^{\mathrm{T}})$.

II. Two-Channel SGFB With Vertex Sampling

Figure 1 shows a two-channel SGFB with vertex domain sampling (SGFBVS) where the subscripts LP and HP refer to the low-pass and high-pass channels of the filter bank, respectively. Based on the results of [15], the filter $\mathbf{H}_{\mathrm{LP}}$ can be obtained as a polynomial function of the normalized adjacency matrix with the order J. Thus, $\mathbf{H}_{\mathrm{LP}} = \frac{1}{2}(\mathbf{I}_{\mathrm{N}} + \boldsymbol{\mathcal{B}})$ where $\boldsymbol{\mathcal{B}} = \sum_{l=1}^{J} w_l(\boldsymbol{\mathcal{A}})^l$ and the weights $\{w_l\}_{l=1}^{J}$ are optimized to achieve a desired filter response. Also, $\mathbf{H}_{\mathrm{LP}}$ can be diagonalized as $\mathbf{H}_{\mathrm{LP}} = \mathbf{U}_0\overline{\mathbf{H}}_{\mathrm{LP}}\mathbf{U}_0^{\mathrm{T}}$ where

$$\overline{\mathbf{H}}_{\mathrm{LP}} = \frac{1}{2}(\mathbf{I}_N + \boldsymbol{\Psi}), \tag{1}$$

$\boldsymbol{\Psi} = \sum_{l=1}^{J} w_l(\mathbf{I}_N - \boldsymbol{\Lambda})^l = \mathrm{diag}\{[\psi_0, \ldots, \psi_{N-1}]^{\mathrm{T}}\}$ with $\psi_n = \sum_{l=1}^{J} w_l(1-\lambda_n)^l$ and $\bar{H}_{\mathrm{LP}}(n) = \frac{1}{2}(1+\psi_n)$. Additionally, $\mathbf{U}_0$ and $\boldsymbol{\Lambda}$ are the eigenvector and eigenvalue matrices of the normalized Laplacian matrix for the original graph, respectively. The high-pass filter $\mathbf{H}_{\mathrm{HP}}$ can be constructed as $\mathbf{H}_{\mathrm{HP}} = \mathbf{I}_{\mathrm{N}} - \mathbf{H}_{\mathrm{LP}}$ [15]. After filtering, the signals $\tilde{\mathbf{f}}_{\mathrm{LP}}$ and $\tilde{\mathbf{f}}_{\mathrm{HP}}$ in low-pass and high-pass channels are downsampled by the factors R_{LP} and R_{HP}, respectively. Therefore, the corresponding graph is reduced. To reduce the graph size, in this letter, we use the well-known Kron reduction method [23]. In the synthesis section, the upsampled signals are combined and the signal $\mathbf{y} = \frac{1}{2}(\mathbf{I}_N + \mathbf{K}\boldsymbol{\mathcal{B}})\mathbf{f}$ in the vertex domain is formed where $\mathbf{K}$ is a diagonal matrix with the diagonal elements $K(i,i) = 1$ if node i is maintained after downsampling at LP channel, otherwise $K(i,i) = -1$. Finally, under the condition that $(\mathbf{I}_N + \mathbf{K}\boldsymbol{\mathcal{B}})$ is invertible, the original signal $\mathbf{f}$ is perfectly reconstructed as $\mathbf{f}_{\mathrm{out}} = \mathbf{H}_{\mathrm{INV}}\mathbf{y}$ where $\mathbf{H}_{\mathrm{INV}} = 2(\mathbf{I}_N + \mathbf{K}\boldsymbol{\mathcal{B}})^{-1}$ [15]. Hence, the weights, w_l, need to be designed to guarantee the invertibility of $(\mathbf{I}_N + \mathbf{K}\boldsymbol{\mathcal{B}})$.

III. Two-Channel SGFB With Spectral Sampling

In this section, we propose a structure for the two-channel SGFB based on the spectral sampling concept which was first introduced in [16], see Fig. 2. We derive PR conditions, present a filter design method and derive a closed-form for the inverse synthesis filter leading to a low complexity implementation.

Let us consider the downsampling matrices as

$$\bar{\mathbf{S}}_{\mathrm{dLP}} = \begin{bmatrix}\mathbf{I}_{N/2} & \mathbf{J}_{N/2}\end{bmatrix}, \bar{\mathbf{S}}_{\mathrm{dHP}} = \begin{bmatrix}\mathbf{I}_{N/2} & -\mathbf{J}_{N/2}\end{bmatrix}, \tag{2}$$

where $\mathbf{J}_{N/2}$ is the counter identity matrix of size $N/2$, [16], [20] and the upsampling matrices as $\bar{\mathbf{S}}_{\mathrm{uLP}} = \bar{\mathbf{S}}_{\mathrm{dLP}}^{\mathrm{T}}$ and $\bar{\mathbf{S}}_{\mathrm{uHP}} = \bar{\mathbf{S}}_{\mathrm{dHP}}^{\mathrm{T}}$. Hence, from Fig. 2, the spectral domain signal $\mathbf{y}$ can be obtained as

$$\mathbf{y} = \big(\bar{\mathbf{S}}_{\mathrm{uLP}}\mathbf{U}_1^{\mathrm{T}}\mathbf{U}_1\bar{\mathbf{S}}_{\mathrm{dLP}}\overline{\mathbf{H}}_{\mathrm{LP}} + \bar{\mathbf{S}}_{\mathrm{uHP}}\mathbf{U}_1^{\mathrm{T}}\mathbf{U}_1\bar{\mathbf{S}}_{\mathrm{dHP}}\overline{\mathbf{H}}_{\mathrm{HP}}\big)\mathbf{U}_0^{\mathrm{T}}\mathbf{f}, \tag{3}$$

where $\mathbf{U}_0$ and $\mathbf{U}_1$ are the unitary eigenvector matrices corresponding to the original and the reduced-size graphs, respectively [16]. Since, $\mathbf{U}_1^{\mathrm{T}}\mathbf{U}_1 = \mathbf{I}_{N/2}$, (3) reduces to

$$\mathbf{y} = \big(\bar{\mathbf{S}}_{\mathrm{uLP}}\bar{\mathbf{S}}_{\mathrm{dLP}}\overline{\mathbf{H}}_{\mathrm{LP}} + \bar{\mathbf{S}}_{\mathrm{uHP}}\bar{\mathbf{S}}_{\mathrm{dHP}}\overline{\mathbf{H}}_{\mathrm{HP}}\big)\mathbf{U}_0^{\mathrm{T}}\mathbf{f}. \tag{4}$$

By substituting (1) and (2) into (4), we have

$$\mathbf{y} = \boldsymbol{\mathcal{C}}\mathbf{U}_0^{\mathrm{T}}\mathbf{f}, \tag{5}$$

where the square matrix $\boldsymbol{\mathcal{C}} = \mathbf{I}_N + \mathbf{J}_N\boldsymbol{\Psi}$ is non-zero only on its main and anti-diagonal elements, i. e.,

$$\boldsymbol{\mathcal{C}} = \begin{bmatrix} 1 & 0 & \cdots & 0 & \psi_{N-1} \\ 0 & 1 & \cdots & \psi_{N-2} & 0 \\ \vdots & \vdots & \ddots & \vdots & \vdots \\ 0 & \psi_1 & \cdots & 1 & 0 \\ \psi_0 & 0 & \cdots & 0 & 1 \end{bmatrix}. \tag{6}$$

From Fig. 2 and using (5), the output signal of the synthesis section can be represented as

$$\mathbf{f}_{\text{out}} = \mathbf{U}_0\overline{\mathbf{H}}_{\text{INV}}\mathbf{y} = \mathbf{U}_0\overline{\mathbf{H}}_{\text{INV}}\boldsymbol{\mathcal{C}}\mathbf{U}_0^{\text{T}}\mathbf{f}. \tag{7}$$

From this equation, one may realize that in contrast to the inverse filter in Fig. 1 that works in the vertex domain, the inverse filter in our proposed structure operates in the spectral domain. Based on (7), the original signal $\mathbf{f}$ can be perfectly reconstructed when $\overline{\mathbf{H}}_{\text{INV}} = \boldsymbol{\mathcal{C}}^{-1}$. Hence, the two-channel SGFBSS has PR property under the condition that $\boldsymbol{\mathcal{C}}$ is invertible. The square matrix $\boldsymbol{\mathcal{C}}$ is invertible if and only if its rows are linearly independent.

Lemma 1: The square matrix $\boldsymbol{\mathcal{C}}$ is invertible and the original signal $\mathbf{f}$ is perfectly reconstructed using (7), if and only if $\psi_n \neq \frac{1}{\psi_{N-n-1}}, \forall\, n \in \{0, \ldots, N/2-1\}$.

Proof: The special structure of the matrix $\boldsymbol{\mathcal{C}}$ that is shown in (6), suggests that this matrix always has $\frac{N}{2}$ independent rows. This is because $\boldsymbol{\mathcal{C}} = [\mathbf{c}_0^{\text{T}}, \ldots, \mathbf{c}_{N-1}^{\text{T}}]^{\text{T}}$ is always comprised of $\frac{N}{2}$ pairs of symmetrical rows, $\mathbf{c}_n$ and $\mathbf{c}_{N-n-1}$ with non-zero entries on the same columns. Hence, this matrix has N independent rows if and only if each pair of symmetrical rows are linearly independent, i.e.,

$$\nexists\, \alpha, \quad \mathbf{c}_n = \alpha\mathbf{c}_{N-n-1}, \quad n = 0, \ldots, N/2-1, \tag{8}$$

where α is a scalar [24]. Let us assume there exists an α so that $\mathbf{c}_n = \alpha\mathbf{c}_{N-n-1}$. From (6) and using (8), one may realize that $\psi_n = \frac{1}{\alpha}$ and $\psi_{N-n-1} = \alpha$. Consequently, the condition in (8) is satisfied by $\psi_n \neq \frac{1}{\psi_{N-n-1}}$. ■

The above lemma shows that we have only $N/2$ constraints for a perfect reconstruction transform which is 4 times smaller than the number of constraints in [20]. This leads to a large amount of flexibility in the choice of filter parameters.

A. Filter Design Methodology

The shape of the filters plays a crucial role for signal decomposition into different spectral bands. In this section, a pair of analysis filters with desirable frequency responses is proposed for SGFBSS. We consider the spectral kernel as

$$\bar{H}_{\text{LP}}(n) = \begin{cases} 1, & \text{if } \lambda_n \leq \lambda_{\text{cut}}, \\ \varepsilon, & \text{if } \lambda_n > \lambda_{\text{cut}}. \end{cases} \tag{9}$$

For $\lambda_{\text{cut}} = \lambda_{\frac{N}{2}-1}$ and $\varepsilon = 0$, we have the exact ideal low-pass filter. Using (1), we have $\psi_n = 2\bar{H}_{\text{LP}}(n) - 1, n = 0, \ldots, N-1$. Hence, for the exact ideal filter, $\psi_0 = \ldots = \psi_{\frac{N}{2}-1} = 1$ and $\psi_{\frac{N}{2}} = \ldots = \psi_{N-1} = -1$. For higher flexibility, the cut-off frequency can be variable within the range $\lambda_0 < \lambda_{\text{cut}} \leq \lambda_{\frac{N}{2}-1}$ and then $\varepsilon \neq 0$ to satisfy the PR condition, as mentioned earlier.

Non-ideal filters are sometimes preferred when the eigenvalue distribution of the variation operator is irregular [20]. As an example of such filters, in this letter, we assume a Butterworth filter with order β as $\bar{H}_{\text{LP}}(n) = (1 + (\lambda_n/\lambda_{\text{cut}})^{2\beta})^{-0.5}$. It is worth noting that the choice of Butterworth filter here is due to its maximally flat spectral response. The cut-off frequency does not have any limitations in our proposed SGFBSS structure. Thus, λ_{cut} and β are the design parameters. The selection of the cut-off frequency for analysis filters in GFBs has received less attention in the literature, [7]–[9], [20]. In GFBs for bipartite graphs, $\lambda_{\text{cut}} = \lambda_{\frac{N}{2}-1}$ is assumed. This is reasonable due to the order of eigenvalues for bipartite graphs. However, the shapes of the filters for arbitrary graphs are important and require more flexibility for cut-off frequency which is satisfied by using our method.

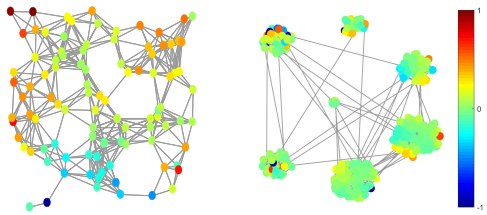

(a) Sensor graph (N=100) (b) Community graph (N=400)

Fig. 3. Graph signal in vertex domain.

B. Low-Complexity Implementation

As it was mentioned in the proof of Lemma 1, $\boldsymbol{\mathcal{C}}$ contains $\frac{N}{2}$ pairs of symmetrical rows, $\mathbf{c}_n$ and $\mathbf{c}_{N-n-1}$ with non-zero elements only on two similar columns. As a result, the linear system of equations in (5) that is defined by the coefficient matrix $\boldsymbol{\mathcal{C}}$, can be broken into $\frac{N}{2}$ isolated linear systems of equations with only two unknowns in each. Consequently, $\boldsymbol{\mathcal{C}}^{-1}$ can be easily obtained by inverting $\frac{N}{2}$ matrices each of size 2×2. Hence, $\boldsymbol{\mathcal{C}}^{-1} = \widetilde{\boldsymbol{\Psi}}(\mathbf{I}_N - \mathbf{J}_N\boldsymbol{\Psi})$ where $\widetilde{\boldsymbol{\Psi}} = \text{diag}\{[\widetilde{\Psi}(0), \ldots, \widetilde{\Psi}(N-1)\}$ is a diagonal matrix with diagonal elements $\widetilde{\Psi}(n) = \widetilde{\Psi}(N-n-1) = 1/(1-\psi_n\psi_{N-n-1})$ for $n = 0, \ldots, N/2-1$ that are reciprocals of the determinants of the corresponding 2×2 matrices. This simple closed-form for $\boldsymbol{\mathcal{C}}^{-1}$, significantly reduces the computational complexity of the matrix inversion especially for large graphs.

To compare the complexity of our proposed SGFBSS structure with other existing solutions in [13], [15], [20], [22], we focus on filtering and sampling. Both the spectral approaches of SGFBSS and the method in [20] have the same complexity for filtering in the analysis section and sampling. Interestingly, both GFBs have the same complexity in the synthesis section. In particular, spectral domain filtering in [20] requires $2\mathcal{O}(N)$ number of multiplications. To pass the signal $\mathbf{y}$ through the inverse filter $\overline{\mathbf{H}}_{\text{INV}}$, our proposed SGFBSS method requires $2\mathcal{O}(N)$ rather than $\mathcal{O}(N^2)$ multiplications as compared with the SGFBVS method in [15] and [22]. However, the class of vertex sampling methods such as the ones in [13], [15] and [22] require lower complexity than methods with spectral sampling such as the one proposed in this letter and [20]. This is the cost to pay for the better performance of the spectral sampling based methods.

IV. Simulation Results

In this section, we evaluate and compare the performance of our proposed SGFBSS structure with the existing GFBs in the literature, [7]–[9], [11]–[13], [20], [22]. We have used GSPbox in MATLAB, [25], for graph generation, GSP operations, and visualizations. Similar to [20], we consider two different graph signals with vertex and spectral representations that are shown in Figs. 3 and 4, respectively. Figs. 4 and 4 illustrate an approximately smooth signal and a localized signal in the spectral domain on the sensor and community graphs, respectively. As mentioned before, we have freedom in choosing the analysis filters and cut-off frequencies. We assume ideal and Butterworth filters depicted in Fig. 5 for the community graph as an example. Fig. 5 and Fig. 5 show the ideal filters with different cut-off frequencies and Butterworth filters with different orders for $\lambda_{\text{cut}} = \lambda_{\frac{N}{2}-1}$, respectively. In the following, the performance of

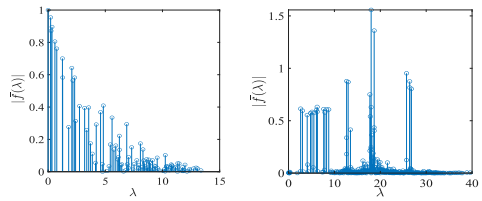

(a) Sensor graph signal (b) Community graph signal

Fig. 4. Graph signal in spectral domain.

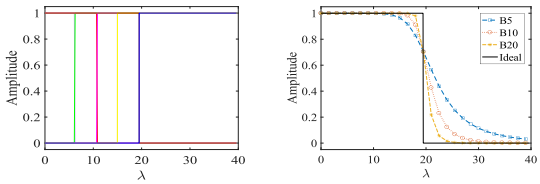

(a) SGFBSS-I (b) SGFBSS-B

Fig. 5. Filter sets for SGFBSS (a) Ideal filters, (b) Butterworth filters.

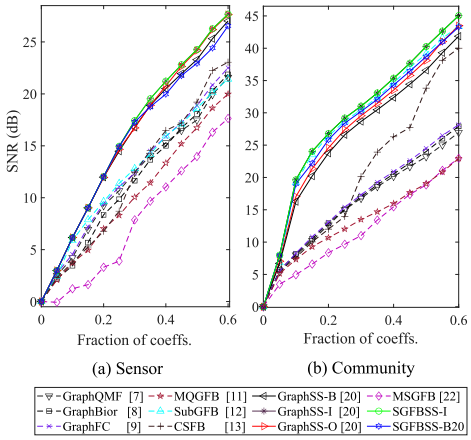

Fig. 6. Results of nonlinear approximation.

our proposed method in nonlinear approximation and denoising is evaluated.

A. Nonlinear Approximation

In nonlinear approximation, a fraction of the coefficients with high absolute values are kept and the rest are set to zero. In Fig. 6, we compare our proposed SGFBSS structure with GraphQMF [7], GraphBior [8], GraphFC [9], MQGFB [11], SubGFB [12], CSFB [13], GraphSS [20] and MSGFB [22]. This figure shows the resulting signal to noise ratio (SNR) versus the fraction of remaining coefficients for both sensor and community graphs. SGFBSS-I and SGFBSS-B20 represent SGFBSS with ideal and order 20 Butterworth filters, respectively. Our results in Fig. 6 show that spectral sampling based methods outperform the ones with vertex sampling that are shown with solid and dashed lines, respectively. In particular, our proposed SGFBSS structure achieves a significantly improved performance compared to its counterpart SGFB with vertex sampling, [22]. Furthermore, while having a superior performance to all the existing methods, our proposed structure leads to about the same performance as GraphSS, [20].

TABLE I
DENOISING RESULTS. AVERAGE OF 1000 RUNS

	Methods	$\sigma = 1/8$	$\sigma = 1/4$	$\sigma = 1/2$	$\sigma = 1$
Sensor	GraphSS-I [20]	0.41	1.28	4.89	10.34
	GraphSS-O [20]	0.37	1.28	4.89	10.40
	GraphSS-B [20]	0.24	1.20	4.84	10.37
	CSFB [13]	0.41	1.28	4.89	10.34
	MQGFB [11]	-2.90	-0.05	4.76	10.20
	SGFBSS-I	0.41	1.28	4.89	10.34
	SGFBSS-B5	0.51	**1.36**	**5.10**	**10.82**
	SGFBSS-B10	**0.52**	1.31	4.96	10.69
	SGFBSS-B20	0.47	1.33	4.94	10.55
Community	GraphSS-I [20]	**6.04**	4.85	7.68	12.11
	GraphSS-O [20]	5.39	4.50	7.53	12.13
	GraphSS-B [20]	5.07	4.40	7.49	11.86
	CSFB [13]	**6.04**	4.85	7.68	12.11
	MQGFB [11]	0.64	3.65	7.12	11.71
	SGFBSS-I	**6.04**	4.85	7.68	12.11
	SGFBSS-B5	3.78	4.06	**7.80**	**13.20**
	SGFBSS-B10	5.28	4.72	7.76	12.72
	SGFBSS-B20	5.94	**4.86**	7.79	12.38

B. Denoising

In this subsection, we evaluate the performance of our proposed SGFBSS structure for noise suppression. We consider the noisy signal $\mathbf{f}_{\text{noisy}} = \mathbf{f} + \boldsymbol{\xi}$ where $\boldsymbol{\xi}$ is the zero-mean white Gaussian noise vector with the standard deviation σ. We compare both SGFBSS-I and SGFBSS-B (with different orders 5, 10, and 20) with MQGFB utilizing "lazy" bi-orthogonal filters [11], CSFB [13] and GraphSS [20]. We use the non-normalized Laplacian matrix as the variation operator. The cut-off frequency is chosen as $\lambda_{\text{cut}} = \lambda_{\frac{N}{2}-1}$ and the coefficients at low and high frequency channels are hard-thresholded with $T = 3\sigma$. Denoising results for the graph signals of Fig. 3 are shown in Tab. I in terms of signal-to-noise ratio (SNR) improvement in dB, i.e., $\Delta_{\text{SNR}} = 10\log_{10}(\frac{\|\boldsymbol{\xi}\|_2^2}{\|\mathbf{f}_{\text{denoised}}-\mathbf{f}\|_2^2})$ [3]. In this table, different noise levels are considered and the largest Δ_{SNR} values are represented in bold. Our results show that in many cases, non-ideal filters outperform the ideal ones. For the sensor graph, our proposed method is superior to all the other methods for different noise levels. Similar results are achieved for the community graph while only for the lowest noise level, $\sigma = 1/8$, our proposed method SGFBSS-I leads to the same performance as the methods in [13] and [20]. Finally, for all the other noise levels, our proposed SGFBSS-B provides the highest SNR improvement.

V. CONCLUSION

In this letter, we introduced a two-channel critically-sampled SGFB structure based on the spectral sampling concept. This structure is applicable to any arbitrary undirected graph and can use both normalized and non-normalized graph Laplacian. We derived the PR conditions and discussed the filter design aspects. Our proposed structure provides a large amount of flexibility in terms of shape and cut-off frequency of the filters. We derived a closed-form for the synthesis filter that led to a low complexity implementation of the synthesis section. Our simulation results demonstrate the superior nonlinear approximation and noise suppression performance of our proposed method compared to the existing GFB structures in the literature.

REFERENCES

[1] D. Shuman, S. Narang, P. Frossard, A. Ortega, and P. Vandergheynst, "The emerging field of signal processing on graphs: Extending high-dimensional data analysis to networks and other irregular domains," *IEEE Signal Process. Mag.* vol. 30 no. 3, pp. 83–98, May 2013.

[2] A. Ortega, P. Frossard, J. Kovačević, J. M. F. Moura, and P. Vandergheynst, "Graph signal processing: Overview, challenges and applications," *Proc. IEEE*, vol. 106, no. 5, pp. 808–828, May 2018.

[3] D. I. Shuman, "Localized spectral graph filter frames: A unifying framework, survey of design considerations, and numerical comparison," *IEEE Signal Process. Mag*. vol. 37 no. 6, pp. 43–63, Nov. 2020.

[4] M. Gavish, B. Nadler, and R. R. Coifman "Multiscale wavelets on trees, graphs and high dimensional data: Theory and applications to semi supervised learning," in *Proc. Int. Conf. Mach. Learn*., 2010, pp. 367–374.

[5] O. Teke and P. P. Vaidyanathan "Extending classical multirate signal processing theory to graphs–Part II: M-channel filter banks," *IEEE Trans. Signal Process*., vol. 65, no. 2, pp. 423.437, Jan. 2017.

[6] V. N. Ekambaram, G. C. Fanti, B. Ayazifar, and K. Ramchandran, "Multiresolution graph signal processing via circulant structures," in *Proc. Digit. Signal Process. Signal Process. Educ. Meeting*, 2013, pp. 112–117.

[7] S. K. Narang and A. Ortega, "Perfect reconstruction two-channel wavelet filter banks for graph structured data," *IEEE Trans. Signal Process.*, vol. 60, no. 6, pp. 2786–2799, Jun. 2012.

[8] S. K. Narang and A. Ortega, "Compact support biorthogonal wavelet filterbanks for arbitrary undirected graphs," *IEEE Trans. Signal Process.*, vol. 61, no. 19, pp. 4673–4685, Oct. 2013.

[9] A. Sakiyama, K. Watanabe, and Y. Tanaka, "Spectral graph wavelets and filter banks with low approximation error," *IEEE Trans. Signal Inf. Process. Netw.*, vol. 2, no. 3, pp. 230–245, Sep. 2016.

[10] A. Sakiyama and Y. Tanaka, "M-channel oversampled graph filter banks," *IEEE Trans. Signal Process.*, vol. 62, no. 14, pp. 3578–3590, Jul. 2014.

[11] E. Pavez, B. Girault, A. Ortega, and P. A. Chou, "Spectral folding and two-channel filter-banks on arbitrary graphs," Jun. 2020.

[12] N. Tremblay and P. Borgnat, "Subgraph-based filterbanks for graph signals," *IEEE Trans. Signal Process.*, vol. 64, no. 15, pp. 3827–3840, Aug. 2016.

[13] S. Li, Y. Jin, and D. I. Shuman, "Scalable M-channel critically sampled filter banks for graph signals," *IEEE Trans. Signal Process.*, vol. 67, no. 15, pp. 3954–3969, Aug. 2019.

[14] A. Anis and A. Ortega, "Critical sampling for wavelet filterbanks on arbitrary graphs," in *Proc. Int. Conf. Acoust. Speech, Signal Process*., 2017, pp. 3889–3893.

[15] V. N. Ekambaram, G. C. Fanti, B. Ayazifar, and K. Ramchandran, "Spline-like wavelet filterbanks for multiresolution analysis of graph-structured data," *IEEE Trans. Signal Inf. Process. Netw.*, vol. 1, no. 4, pp. 268–278, Dec. 2015.

[16] Y. Tanaka, "Spectral domain sampling of graph signal," *IEEE Trans. Signal Process.*, vol. 66, no. 14, pp. 3752–3767, Jul. 2018.

[17] Y. Tanaka, Y. C. Eldar, A. Ortega, and G. Cheung, "Sampling on graphs: From theory to applications," *IEEE Signal Process. Mag*. vol. 37, no. 6, pp. 14–30, Nov. 2020.

[18] J. Z. Jiang, C. Cheng, and Q. Sun, "Nonsubsampled graph filter banks: Theory and distributed implementation," *IEEE Trans. Signal Process.*, vol. 67, no. 15, pp. 3938–3953, Aug. 2019.

[19] J. Z. Jiang, D. B. Tay, Q. Sun, and S. Ouyang, "Design of nonsubsampled graph filter banks via lifting schemes," *IEEE Trans. Signal Process. Lett.*, vol. 27, pp. 441–445, 2020.

[20] A. Sakiyama, K. Watanabe, Y. Tanaka, and A. Ortega, "Two-channel critically sampled graph filter banks with spectral domain sampling," *IEEE Trans. Signal Process.*, vol. 67, no. 6, pp. 1447–1460, Mar. 2019.

[21] A. Sakiyama, K. Watanabe, and Y. Tanaka, "M-channel critically sampled spectral graph filter banks with symmetric structure," *IEEE Trans. Signal Process. Lett.*, vol. 26, no. 5, pp. 665–669, May 2019.

[22] A. Miraki and H. Saeedi-Sourck, "A modified spline graph filter bank," *Circuits Syst. Sig. Process*., Sep. 2020.

[23] F. Dorfler and F. Bullo, "Kron reduction of graphs with applications to electrical networks," *IEEE Trans. Circuits Syst. I, Reg. Papers*, vol. 60, no. 1, pp. 150–163, Jan. 2013.

[24] R. A. Horn and C. R. Johnson, *Matrix Analysis*, 2nd ed. New York, NY, USA: Cambridge Univ. Press, 1990.

[25] N. Perraudin, J. Paratte, D. Shuman, V. Kalofolias, P. Vandergheynst, and D. K. Hammond, "GSPBOX: A toolbox for signal processing on graphs," Aug. 2014, *arXiv:1408.5781*.